JOURNAL OF OPTOELECTRONICS AND ADVANCED MATERIALS, Vol. 11, No. 4, April 2009, p. 515 – 519

Characterization of a novel 1,3-bis-(p-iminobenzoic acid) indane Langmuir-Blodgett (LB) films containing Cd^{2+} ions in Langmuir-Blodgett (LB) films

T. UZUNOĞLU, H. SARI*, R. ÇAPAN[a], H. NAMLI[b], O. TURHAN[b]
Ankara University, Faculty of Engineering, Department of Engineering Physics, 06100 Tandogan, Ankara, Turkey
[a]*Balikesir University, Faculty of Science, Department of Physics, 10100 Balikesir, Turkey*
[b]*Balikesir University, Faculty of Science, Department of Chemistry, 10100 Balikesir, Turkey*

Newly synthesized 1,3-bis-(*p*-iminobenzoic acid) indane and 1,3-bis-(*p*-iminobenzoic acid) indane incorporating Cd^{2+} films were grown Z-type onto aluminum coated glass substrates by Langmuir-Blodgett film (LB) technique. The transferred 1,3-bis-(*p*-iminobenzoic acid) indane molecules and the molecules incorporating Cd^{2+} ions onto substrate were verified by UV-visible absorption spectra and layer by layer growth was confirmed by quartz crystal microbalance (QCM) technique. Electrical properties of the different layered films were investigated by measuring room temperature I-V curves. By analyzing I-V curves and assuming Schottky conduction mechanism the barrier height values have been calculated for LB films with different number of layers.

(Received April 1, 2009; accepted April 23, 2009)

Keywords: Langmuir-Blodgett thin films, 1,3-bis-(*p*-iminobenzoic acid) indane, Cd^{2+} ion, QCM

1. Introduction

Langmuir-Blodgett (LB) film technique is very convenient method to produce nanostructure films with high level structures and the thickness of the LB film can be easily controlled at molecular level [1, 2]. In this technique the size of the nanoparticles in the films mainly depends on the organic molecules in which it was grown as well as the growth procedure.

Group II-VI semiconductor nanoparticles were increasingly used in optoelectronic applications. When the spatial dimensions of such semiconductors are reduced further additional quantum effects, such as quantum confinement can be observed. Recently it was successfully demonstrated that organic thin films containing nanoparticle form of group II-VI compound semiconductors, including cadmium sulphide (CdS) [3] and zinc sulphide (ZnS) [4] can be formed within organic multilayer thin film using Langmuir-Blodgett (LB) deposition technique. In order to understand the process of growing good quality of these nanoparticles it is essential understand the interaction between metal ions and organic films. The interaction between the Langmuir layers of fatty acids and metal ions has been studied since 1980s [5, 6]. Watanabe et al. [7] studied the interactions between a conducting LB films and different transition-metal ions (Ni^{2+}, Cd^{2+}, Cu^{2+}, and Zn^{2+}) for chemical sensors. Jung et al. [8] investigated electrical properties for the monolayers LB films of pure G4-48PyP dendrimer and its complex with metal ions (Pt^{4+} and Fe^{2+} ions). The *I–V* characteristics of metal/dendrimer LB film/metal and metal/dendrimer LB film with complex metal ions/metal sandwich structures were measured. Results of I-V measurement showed that there is a difference between pure G4-48PyP dendrimer LB film and its complex metal ions [8].

The pyroelectrical activity in copolysiloxane/eicosylamine alternate layer Langmuir–Blodgett (LB) films incorporating Cd^{2+} and Mn^{2+} ions was also reported and the pyroelectric results showed that cadmium ion incorporation caused a considerably improved performance compared to the system without metal ions [9].

In this study, Z-type LB films of 1,3-bis-(*p*-iminobenzoic acid) indane (IBI) and 1,3-bis-(*p*-iminobenzoic acid) indane (IBI) containing Cd^{2+} films have been deposited onto aluminum substrate to fabricate a metal/Z-type LB film/metal device in order to investigate influence of Cd^{2+} ions on electrical properties of 1,3-bis-(*p*-iminobenzoic acid) indane molecules.

2. Experimental details

The chemical structure of 1,3-bis-(*p*-iminobenzoic acid) indane (IBI) molecule is shown in Fig. 1. It was dissolved in a 9:1 ratio of chloroform and methanol. The cadmium chloride ($CdCl_2$) was dissolved in the subphase and 0.5 mg ml^{-1} concentration of solution was used to take an isotherm and to produce LB film by spreading on the pure water surface.

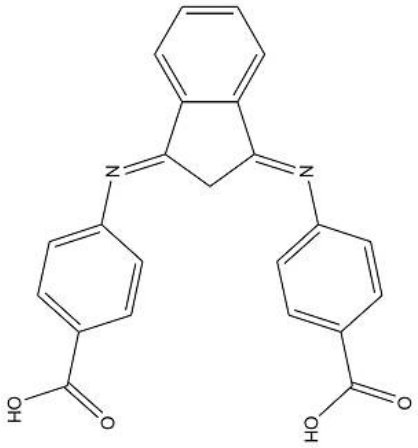

Fig. 1. Chemical structure of 1,3-bis-(p-iminobenzoic acid) indane

A time period of 15 minutes was allowed for the solvent to evaporate before the area enclosed by the barriers was reduced. The π-A isotherm graph of IBI was recorded as a function of surface area at pH 6.0 and the compression speed for the monolayer was controlled at 1000 mm min^{-1}. Isotherm graph given in Fig. 2 was repeated several times and the results were found to be reproducible. Using the isotherm graph, the deposition pressure of 20 mN/m is selected to produce Z-type LB films in the thickness of 5, 15, and 25 monolayer for optical and electrical measurement and 5, 11, 15, 21, and 25 monolayer for quartz crystal microbalance (QCM) measurements by vertically dipping substrates to the solution. The temperature of the water subphase was controlled using Lauda Ecoline RE 204 model temperature control unit and all experimental data were taken at room temperature.

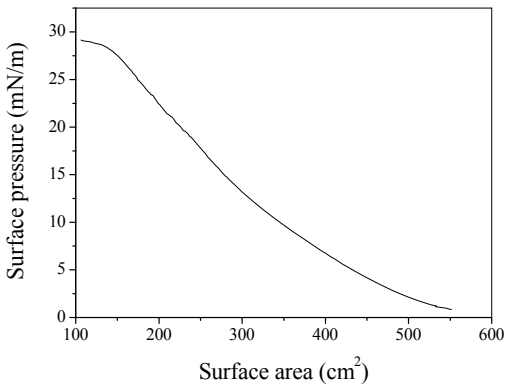

Fig. 2. Isotherm graph of 1,3-bis- (p-iminobenzoic acid) indane monolayer incorporation of cadmium ions

It is well known that cadmium ions interact with carboxylic acid head groups (COO^-) and thus the ions can easily accommodate in a multilayer LB film structure [10]. The schematic diagram of the incorporation of Cd^{+2} ions in IBI molecule is shown in Fig. 3.

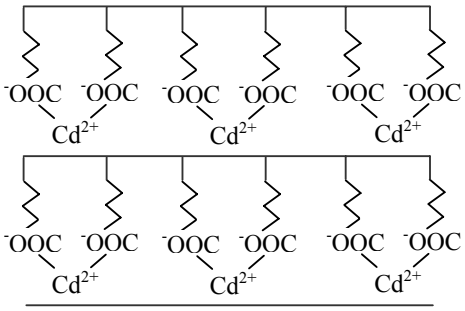

Fig. 3. Schematic diagram of alternate 1,3-bis-(p-iminobenzoic acid) indane incorporating Cd^{+2} films layer structure.

In order to verify layer by layer growth a thiny cut wafer of raw quartz sandwiched between two electrodes in an overlapping keyhole design was used for the QCM measurements. QCM measurements were performed at room temperature using an in-house designed oscillating circuit and standard quartz crystal with a nominal resonance frequency of 9 MHz. The frequency was measured with a Motech FG-513 model function generator and Tektronix TDS 210 model digital oscilloscope.

In this study, microscope glass and aluminised microscope glass were used for optical and electrical measurements, respectively. The films were grown on Al-coated glass placed into a thermal evaporator for top electrode fabrication. Top electrodes were fabricated under 8×10^{-7} mbar vacuum by evaporating aluminium using a mask which has 16 parallel; 1mm×15mm sized opening interdigitated grids on it. Metal/LB films/metal sandwich structure is shown Fig. 4.

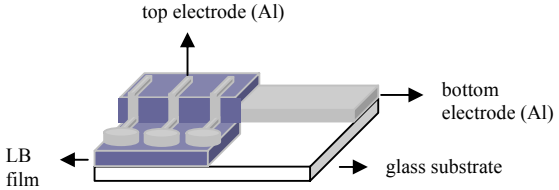

Fig. 4. The device structure of LB film for electrical measurements

Optical measurements were carried out with Perkin Elmer Lambda-2 UV-Vis spectrometer. For electrical measurements HP 4192A impedance analyzer, Keithley 228A current source, Keithley 6514 voltmeter, and Keithley 485 ampermeter were used. All the data was taken automatically by using a GPIB interface card and Labview data acquisition software.

3. Experimental results

Fig. 5 shows the frequency change of the quartz crystal during the trasfer IBI molecules containing Cd^{2+} ions onto QCM plate by the vertical lifting methods. 5, 11, 15, 21, and 25 monolayer transferred onto the QCM and change in frequencies were meassured. Fig. 5 shows a plot of the change in the resonant frequency change against the number of deposited layers for all the samples. The frequency change vs. number of layer curve shows linear behaviour regardless.

In an attempt to determine the quality of LB film multilayers on the QCM crystal, the relationship between the frequency change and mass is investigated. A quartz crystal with electrodes on both sides resonates at an extremely well-defined frequency when placed in a suitable electronic control unit. The resonant frequency depends on the area of the electrode and thickness of the quartz crystal. The resonant frequency of the crystal is extremely sensitive to small mass changes. The change in resonant frequency, Δf has been shown to be directly proportional to the mass deposition on the quartz crystal. In LB films, Δf should be related directly to the mass of the bilayer and the change in resonant frequency for LB films may be written by [11]

$$\Delta f = \frac{2 f_o^2 \Delta m}{K_q} N \qquad (1)$$

where f_o is the initial oscillation frequency, ρ_q is the density of piezoelectric slab, ν_q is the propagation speed of acoustic waves in the quartz, N is the number of deposition layers, Δm is the mass per unit area per layer, and $K_q = \rho_q \nu_q$.

Table 1. QCM frequency change before and after H_2S exposure

Number of layers	Frequency change (Hz)	Mass change (ng)
5	57.44	66.05
11	97.64	112.29
15	132.11	151.92
21	235.49	270.82
25	310.16	356.69

It is clear from Fig. 5 that the linear relationship confirms the transfer process of the LB film is highly reproducible. This linear relationship suggests that equal mass per unit area is deposited onto the quartz crystal during the transfer of each bilayer. Using Eq. 1 the frequency changes have been calculated for all samples. The calculated values for the samples are given in Table 1.

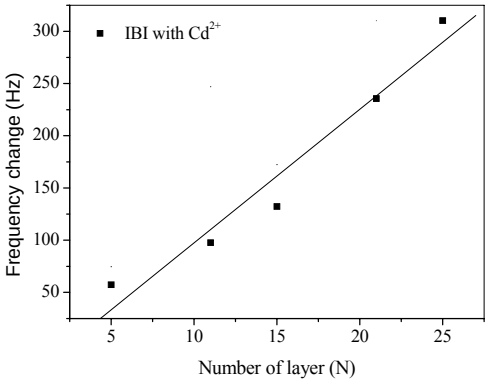

Fig. 5. Room temperature frequency change vs. number of monolayers graph of the LB films.

Fig. 6 shows the UV absorption spectra of the 25 monolayer IBI and IBI containing Cd^{2+} samples. Incorporation of Cd^{2+} ions in the films was verified using UV-Vis spectra method. The absorption peaks of the film remained unchanged, but the overall absorption of the samples containing Cd^{2+} film is increased due to the Cd^{2+} ions.

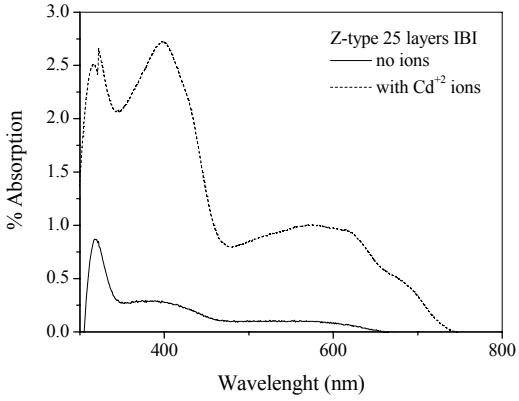

Fig. 6. UV absorption spectra with/without Cd^{2+} for 25 layers IBI films.

The electrical properties of the films are also investigated by measuring room temperature I-V characteristics. Fig. 7 shows I-V curves of the samples. I-V curves show exponential behaviour and regardless of film thickness, there is an increase in current value for the IBI film containing Cd^{2+} ions with respect to the IBI films.

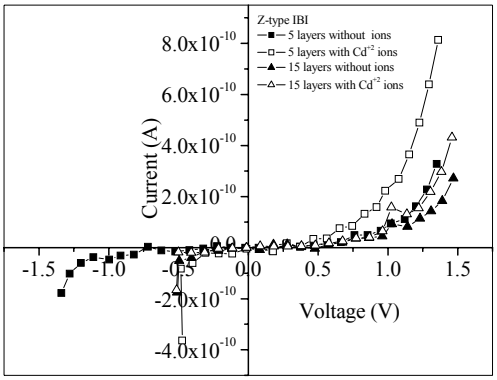

Fig. 7. Room temperature I-V graph of the films IBI (■, ▲) and IBI containing Cd^{2+} (□, Δ)

Although this increase is small it is consistent with the other reported results observed for G4-48PyP dendrimer LB films and its Fe^{2+} ions [8].

In order to explain the conduction process through LB films and the effect of the Cd^{2+} ions on conductivity lnJ versus $V^{1/2}$ has been replotted in Fig. 8 for 5 and 15 layer thick samples in the voltage range corresponding to the exponentially increasing current. As seen from Fig. 8 the relation between lnJ and $V^{1/2}$ shows rather linear dependence.

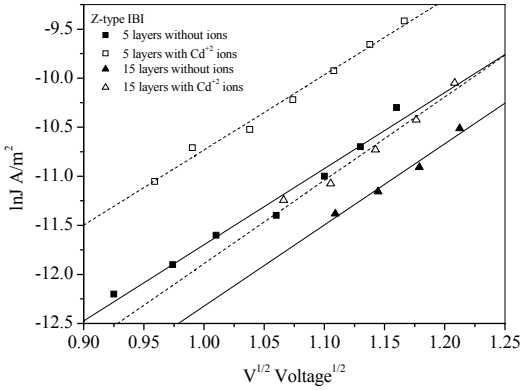

Fig. 8. Plot of lnJ vs $V^{1/2}$ for various number of IBI layers (■, ▲) and IBI containing Cd^{2+} (□, Δ).

The linear dependence suggests that conduction is governed by either Poole-Frankel or Schottky mechanism [12]. We can make basic assumptions and extract some physically acceptable information. If we assume, conduction is governed by Schottky conduction mechanism, which is given by [13]

$$I_{Schottky} = A.S.T^2 \exp\left(\frac{-e\varphi}{kT} + \beta V^{1/2}\right) \quad (2)$$

where A is the Richardson constant, S is the metal contact area, T is absolute temperature, e is the electronic charge, k is the Boltzmann's constant, φ is the potential barrier, V is the applied voltage, and β is the Poole-Frankel field-lowering coefficients given by

$$\beta_{PF} = \frac{e}{kT}\left(\frac{e}{\pi\varepsilon_0\varepsilon_r d}\right)^{1/2} \quad (3)$$

Here ε_r is the dielectric constant of the films; ε_o is the permittivity of free space, d is the film thickness.

The intercept of the linear curve with the lnJ axis at V=0 can be expressed in terms of barrier height (φ) and temperature using Eq.2:

$$\ln J = \ln\left(AT^2\right) - \left(\frac{e}{kT}\right)\varphi \quad (4)$$

The result of the barrier height calculation for the 5 and 15 monolayer thick samples with and without Cd^{2+} ions are summarized in Table 2. The 5 and 15 monolayer thick IBI containing Cd^{2+} samples have slightly different (lower) barrier height than the 5 and 15 monolayer thick IBI samples [8]. Similar results are also reported for the IBI samples containing Zn^{2+} ions grown by LB technique [14]. The presence of the Cd^{2+} ions influences the barrier height at the metal-organic film interface and causes a change in electrical conduction properties of LB films.

Table 2. Calculation details for barrier height energy

Molecules	Number of layers	lnJ (V=0)	Barrier height φ (eV)
IBI	5	-19.48	1.13
	15	-20.18	1.15
IBI containing Cd^{2+}	5	-18.41	1.11
	15	-19.82	1.14

4. Conclusion

IBI molecule and IBI molecules containing Cd^{2+} ions, which are useful for growing semiconductor nanostructures such as CdS were grown in various thicknesses on both glass and aluminized substrates with LB technique. Layer by layer growth was verified by QCM technique. The samples, which have different number of layers, were also verified by UV-Vis absorption spectra. The films containing Cd^{2+} ions have higher current values than the films without Cd^{2+} ions. By assuming Schottky conduction mechanism the average LB film/barrier height was found to be as 1.13 eV for IBI containing Cd^{2+} samples and 1.14 eV for IBI samples, respectively.

Acknowledgements

Financial support from Ankara University Research Office (BAP) (Project code: AU-BAP 2003-07-45-016) is gratefully acknowledged.

References

[1] G. G. Roberts 1990. Langmuir-Blodgett Films, New York, Plenum Press.
[2] M. C. Petty, 1996. Langmuir-Blodgett Films: An Introduction, Cambridge, Cambridge University Press.
[3] Samokhvalov, R.W. Gurney, M. Lahav, S. Cohen, H. Cohen, R. Naaman, J. Phys. Chem. B **107,** 4245 (2003).
[4] C. Tiseanu, R. K. Mehra, R. Kho, M. Kumke, J. Phys. Chem. B **107**, 12153 (2003).
[5] I. R., Peterson, G. J. Russell, Thin Solid Films, **134**, 143 (1985).
[6] M. R. Buhaenko, M. J. Grundy, M. R. Richardson, S. J. Roser, Thin Solid Films, **159,** 253 (1988).
[7] N. Watanabe, H. Ohnuki, M. Izumi, T. Imakub,. Colloids and Surfaces A: Physicochem. Eng. Aspects **284**–**285**, 640 (2006).
[8] S. B. Jung, C. Kim, Y. S., Kwon. Thin Solid Films, **438-439**, 27 (2003).
[9] R. Capan, T. Richardson, D. Lacey, Thin Solid Films, **327-329**, 369 (1998).
[10] E. S. Smotkin, C. Lee, A. J. Bard, M. A. Campton, T. E. Mallok S. E. Webber, J. M.White, Chemical Physics Letters **152**, 265 (1998).
[11] G. Sauerbrey, Z. Phys. **155**, 206 (1959).
[12] N. J. Geddes, J. R. Sambles, W. G. Parker, N. R. Couch, D. J. Jarvis,. J. Phys. D. Appl. Phys., **23,** 95 (1990)
[13] S. M. Sze, 1981. Physics of Semiconductor Devices, Wiley-Interscience, New York, p.250.
[14] H. Sari, T. Uzunoglu, R. Capan, N. Serin, T. Serin, C. Tarimci, A. K. Hassan, H. Namli, O. Turhan, Journal of Nanoscience and Nanotechnology **7**(1-5), 2007.

*Corresponding author: hsari100@gmail.com